



# Gas sensor using surface plasmon resonance, a simulations-based study

*Sensor de gases usando resonancia de plasmón de superficie, un estudio fundamentado en simulaciones*

Edinson Leonardo-Gélvez; Jorge-Enrique Rueda; Luis-Alfonso Guerra

Departamento de Física, Grupo Óptica Moderna, Universidad de Pamplona, Colombia

Correspondencia: edinson2896@gmail.com / jruedap2003@unipamplona.edu.co / chyrry44@gmail.com

Recibido: Abril, 2022. Aceptado: Junio, 2022. Publicado: Julio, 2022

## Resumen

Los plasmones superficiales propagantes son oscilaciones colectivas de los electrones presentes en superficies de film metálica, con los cuales es posible acoplar luz de un haz incidente. En el siguiente trabajo, presentamos una revisión teórica soportada con simulaciones, de los fundamentos físicos de la resonancia de plasmón de superficie usando sistemas Dieléctrico/película Au/Dieléctrico o Dieléctrico/película Ag/Dieléctrico. Estudiamos las posibilidades de la implementación de un sensor de gases usando estos dos tipos de estructuras.

**Palabras clave:** Plasmonica, resonancia de plasmón superficial, detección óptica, campo evanescente.

## Abstract

The propagating surface plasmons are collective oscillations of the electrons present on metallic film surfaces, with which it is possible to couple light from an incident beam. In the following work, we present a simulation-supported theoretical review of the physical foundations of surface plasmon resonance using Dielectric/Au film/Dielectric or Dielectric/Ag film/Dielectric systems. We study the possibilities of implementing a gas sensor using these two types of structures.

**Keywords:** Plasmonic, Surface plasmon resonance, optical sensing, evanescent field.

## 1. Introduction

Electromagnetic waves can be confined in a space or move freely in the metal, if they are in isolated or continuous structures, these are called Localized Surface Plasmons (LSP) and Propagating Surface Plasmons (PSP) [1]. A plasmon corresponds to the collective oscillation of free electrons in a noble metal. Surface plasmons are collective oscillations of electrons that take place at the interface between two media that have dielectric constants of opposite signs, typically a metal (e.g. Au or Ag) and a dielectric (e.g. glass, air or H<sub>2</sub>O).

The most important work to understand the nature of surface plasmons is possibly what was presented in the mid-20th century by Ritchie, who used Maxwell's equations to show that an electromagnetic wave (with transverse magnetic or p-type polarization) can exist and confined to an interface between a metal and a dielectric [2], the amplitude of this decays exponentially towards the interior of the dielectric, the length of the decay wave depends on the wavelength of the incident field and the optical properties of the metal. As a consequence, the excitation will largely depend on the dielectric constant of the medium [3]. Surface plasmon oscillations can be excited by an electrical (electrons) or optical (light) stimulus. However, the excitation cannot be done by directly influencing light on the metal surface because the photon wave vector is always smaller

than that the plasmons ones, the plasmon scattering curve will always be below the curve of dispersion of the photons propagating in the dielectric and for the plasmonic excitation to take place it is necessary that both wave vectors are equal. To meet the resonance condition, different techniques have been used, e.g. Otto's configuration or Kretschmann's configuration [4].

The plasmonic resonance sensors, they essentially measure changes in the refractive index in the medium close to the metal surface that translates into a change in the resonance angle [3]. Therefore, knowing the excitation conditions of surface plasmons, the (effective) thickness can be obtained given the refractive index, or vice versa. These conditions are fulfilled for any metal that allows the free behavior of electrons, for example, gold, silver, copper or aluminum. However, gold or silver film is most often used.

### 1.1 Propagating surface plasmons in metallic systems[30]

Plasmonics is a branch of optics that has been growing in recent years and its study is based on the optical properties of noble metals in nanometric dimensions. This growth can be understood from the advances in nanoscience and nanotechnology, especially in the implementation of new

methods of fabrication and characterization of samples at the nanometric scale.

### 1.2 Optical properties of noble metals<sup>[30]</sup>

Noble metals such as gold and silver are known for their particular dielectric properties that allow them, among other things, to reflect light very efficiently in the visible region of the electromagnetic spectrum. This and other properties have their origin in the presence of free conduction electrons that move in a crystal of positive ions that give charge neutrality. This system of conduction free electrons can, under certain conditions, behave like a plasma of free electrons and its optical response is what governs the optical behavior of the metal. The description of this system in first approximation is done assuming free electrons not interacting with each other, according to the Drude's model. [5,6] In this sense, when an electromagnetic wave strikes a metallic film, the following phenomena occur: reflection, propagation and transmission. [7, 8]

The optical properties of a material depend on the behavior of the electrons within it in the presence of an electric field. In the Drude's model, the metal is modeled as a cloud of free electrons, with a certain density  $N$  and mass of the electron subjected to an external force produced by the electric field and damping due to the collisions between the electrons. Drude's model allows us to visualize that the dielectric function of a metal is composed of a real and an imaginary part. A great advantage of using the Drude's model is that the resolution of Maxwell's equations can be incorporated through solutions by numerical methods. The equation describing the motion of the electron in the material can be written as:

$$m \frac{d^2x}{dt^2} + \beta \frac{dx}{dt} + \kappa_s x = -eE_x, \quad (1)$$

where  $m$  and  $e$  are the mass and charge of the electron,  $\beta$  is the damping coefficient that describes the energy loss due to scattering,  $\kappa_s$  is a constant that describes the restoring force as a consequence of the electrostatic attraction between the atom and the electron. In the case of dielectric materials, electrons fill the valence band and only low-energy transitions between bands are allowed. If the incident field is assumed to be less than that required to induce an electronic transition, the material is directly described by Eq.(1). Solving this equation it is possible to find the real part ( $\epsilon_1$ ) and the imaginary part ( $\epsilon_2$ ) of the dielectric function, for both cases (dielectrics and metals) according to the following procedure: [6,9] given that the electric field  $E_x$  it is harmonic,  $E_x = E_0 e^{(-i\omega t)}$ , Eq. (1) can be written as:

$$\frac{d^2x}{dt^2} + \gamma \frac{dx}{dt} + \omega_0^2 x = \frac{-eE_0 e^{-i\omega t}}{m}, \quad (2)$$

Where  $\beta = \gamma m$ ,  $\kappa_s = \omega_0^2 m$ ,  $\omega_0$  corresponds to the resonance frequency of the electrons bound to the dielectric medium,  $\omega$  is the angular frequency and  $\gamma$  is the damping factor. To find the solution, we assume a solution of the form:

$$x(t) = A e^{-i\omega t} \quad (3)$$

Substituting Eq. (3) in Eq. (2) and solving, we have:

$$A = -\frac{eE_0}{m} \frac{1}{\omega_0^2 - \omega^2 - i\gamma\omega} \quad (4)$$

And

$$x(t) = -\frac{eE_0}{m} \frac{e^{-i\omega t}}{\omega_0^2 - \omega^2 - i\gamma\omega} \quad (5)$$

The displaced electrons contribute to the macroscopic polarization  $P$ . Therefore, the total polarization per unit volume is:

$$P = \frac{\omega_p^2}{\omega_0^2 - \omega^2 - i\gamma\omega} \epsilon_0 E_0 e^{-i\omega t} \quad (6)$$

Where  $\omega_p$  is the plasma frequency,  $n$  is the electron density, and  $\epsilon_0$  is the dielectric constant of vacuum.

$$\omega_p^2 = \frac{Ne^2}{m\epsilon_0} \quad (7)$$

Polarization is related to the electric field through electrical susceptibility  $\chi$ ,

$$P = \chi \epsilon_0 E \quad (8)$$

Then you have:

$$\chi = \frac{\omega_p^2}{\omega_0^2 - \omega^2 - i\gamma\omega} \quad (9)$$

Then the dielectric function can be written as:

$$\epsilon(\omega) = 1 + \chi = 1 + \frac{\omega_p^2}{\omega_0^2 - \omega^2 - i\gamma\omega} = \epsilon_1(\omega) + i\epsilon_2(\omega) \quad (10)$$

where the real and imaginary parts for dielectrics are given by:

$$\epsilon_1(\omega) = 1 + \frac{\omega_p^2(\omega_0^2 - \omega^2)}{(\omega_0^2 - \omega^2)^2 + \gamma^2\omega^2} \quad (11)$$

$$\epsilon_2(\omega) = \frac{\omega_p^2\gamma\omega}{(\omega_0^2 - \omega^2)^2 + \gamma^2\omega^2} \quad (12)$$

For metals,  $\omega_0 = 0$  and substituting this value in Eqs. (11) and (12), the real and imaginary parts are modeled as follows:

$$\epsilon_1(\omega) = 1 - \frac{\omega_p^2}{\gamma^2 + \omega^2} \quad (13)$$

$$\epsilon_2(\omega) = \frac{\omega_p^2\gamma}{\omega(\omega^2 + \gamma^2)} \quad (14)$$

In Fig.1 the real and imaginary parts of the dielectric function are represented graphically, for the parameterization the expression was used:

$$\epsilon = 1 + \frac{C_1}{1 - X^2 - iC_2X} \quad (15)$$

Where  $C_1 = \frac{n^2 e^2}{m\epsilon_0\omega_0} = 0.5$ ,  $C_2 = \frac{\gamma}{\omega_0} = 0.1$ ; Eq.(15) is the same Drude's expression but expressed in terms of  $C_1$ ,  $C_2$  y  $X$ . From this figure it can be seen that the resonant absorption is reflected in the imaginary part of the dielectric function as an absorption peak centered at the resonance frequency and with a width proportional to the damping.

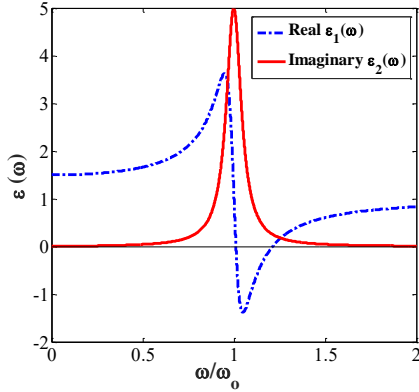


**Figure 1.** Real and imaginary part of the dielectric function, with values:

$$\frac{N^2 e^2}{m \epsilon_0 \omega_0} = 0.5 \quad \text{and} \quad \frac{\gamma}{\omega_0} = 0.1.$$

For low frequencies (below resonance), the real part tends to a constant that reflects the fact that the mechanism in question is able to respond to the field and contribute to the polarization of the medium. When there is an approximation to the resonance frequency, the real part has a maximum that reflects the resonant increase in displacement. Above the resonance frequency, a negative zone appears (for which the refractive index increases with frequency). These zones are called normal scattering zones, where waves cannot propagate through the medium. That is, the negative real part of the dielectric function implies that the material will prevent the penetration of the wave, resulting in a strong reflectivity. Only around the resonance frequency is there an anomalous dispersion zone in which the derivative of the normal part of the dielectric constant with respect to frequency is negative.

### 1.3 Types of surface plasmons

Plasmonics is a branch of nanophotonics that is based on the study of interaction processes between electromagnetic radiation and free conduction electrons in metal-dielectric interfaces. The behaviors observed as a consequence of this interaction can be interpreted based on the existence of plasmons present in a Drude-type metal that have characteristics related to the metal, its geometry, its dimensions, the wavelength of illumination and the surrounding medium. The foundations of plasmonics are laid at the beginning of the 20th century with theoretical works by A. Sommerfeld [10] and experimental observations by R.W. Wood [11], advances in fabrication techniques at 100-nm scales, high-sensitivity characterization methods, the substantial increase in computing power of today's computers, and their wide potential for applications have led to a widespread expansion in interest in this topic. [12] There are two types of surface plasmons: propagating and localized. The propagating types, denoted as SPP, are produced at the flat boundary between a metal and a dielectric, as a consequence of the collective oscillation of the free electrons

of the metal close to its surface. [6,13] This collective oscillation generates an electromagnetic wave that propagates along the interface between both media, generating a very intense electromagnetic field, whose maximum intensity is located at the metal-dielectric interface and decays exponentially on both sides. This. Another type of surface plasmons are localized surface plasmons (LSPs). This type of plasmons are generated in metallic nanostructures (nanoparticles or ordered metallic structures, among others). [7, 9, 14]

#### 1.3.1 Localized surface plasmons

As its name indicates, in this case the LSPs does not spread but it is localized in the region of the nanostructure. [14] The formation of polarizing charges on the nanoparticle surface and the Coulomb attraction between electrons and metal cations act as a restoring force for electrons when they are unbalanced. An amplified resonant field is located within the nanoparticle, resulting in strong light scattering and near-field enhancement at the metal surface. LSPs have the characteristic of being sensitive to the size and shape of the nanoparticle or nanostructured metal surface, which makes it possible to adapt their resonance energy. [9]

#### 1.3.2 Propagating surface plasmons

In an infinite and isotropic conductor, the concept of plasmon can be understood from a classical point of view as collective oscillations of the electrons in the metal. [5,6] In the case of a metallic interface, the electrons oscillate creating a variation in the charge density. From Maxwell's equations [16] it can be found that the possible range of oscillation frequencies varies from  $\omega = 0$  to  $\omega = \omega_p/\sqrt{2}$ , that is, surface plasmons are excited at frequencies below  $\omega_p$ . In Fig.2 the main characteristics of the propagating surface plasmon are shown: a) diagram of the distribution of charge and electric field associated with the propagating surface plasmon; b) distribution of the electric field perpendicular to the surface ( $E_z$ ).  $\delta_m$  and  $\delta_d$  are the penetration length of the electric field in the metal and dielectric, respectively. These longitudinal surface charge oscillations give rise to an electric field, which decays exponentially with distance perpendicular to the surface. This corresponds to an evanescent field with a decay length similar to the wavelength of light. In metals, the surface plasmon exists as charge fluctuations with dimension  $\delta_m$ , which for a wavelength in the near infrared is of the order of 20 nm (this value changes as the frequency increases or is blue shifted). [17, 18]

Considering the dielectric constant  $\delta_m$  for the metal and  $\delta_d$  for the dielectric, the moment along the surface of the propagating surface plasmon is found [19]:

$$\kappa = \left(\frac{\omega}{c}\right) \sqrt{\frac{\epsilon_m \epsilon_d}{\epsilon_m + \epsilon_d}} \quad (16)$$

This solution is given for an electromagnetic wave interacting with the metal surface.

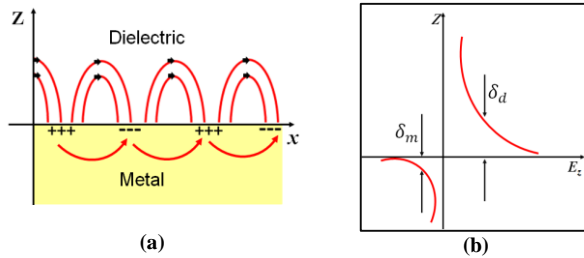


Figure 2. Setup for generation of surface plasmons.

Fig.3 are two illustrations that represent two positions of angle of incidence of the light beam, one where there is no plasmon excitation (Fig.3(a)) and the second position when the precise angle of plasmon excitation is adjusted (Fig.3(b)), which will be observed just when the reflectivity drops sharply, due to the strong absorption of the light beam, a consequence of the resonance between the plasmon and the evanescent wave.

Fig.4 shows the scattering relations for the propagating surface plasmon (solid red curve), for light in vacuum (dashed black line), for light in glass (dashed magenta line). The dotted green line represents the maximum value that the SPP dispersion can reach. It can be seen from the graph that SPPs do not couple directly to an electromagnetic field incident from a vacuum, because the wave vector of light propagating in air is very small compared to the wave vector of the plasmon.

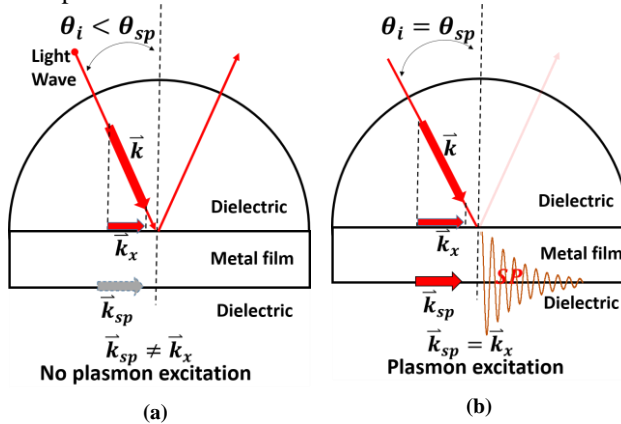


Figure 3. Setup for generation of surface plasmons.

To solve this, the prism coupling method is necessary, which has been widely used to study the properties of SPPs. [17] With this method the light is reflected internally from the base of the glass. In this case, the electromagnetic field inside the glass has a higher momentum than in a vacuum, which can excite an SPP mode (see the point on the graph that indicates the coupling between light and SPP

modes).[9,18,20] To simulate the SPP scattering relationship, Eq.(16) vs corresponding  $\omega$  was used and the scattering relationship for light in vacuum and glass was used with the expression  $\omega = ck$ ,  $c$  is the speed of light in a vacuum and  $k$  is the wave vector of light. For larger values of  $k$ , the SPP spread tends to a constant maximum value of  $\omega_p/\sqrt{2}$  becoming independent of  $k$ .

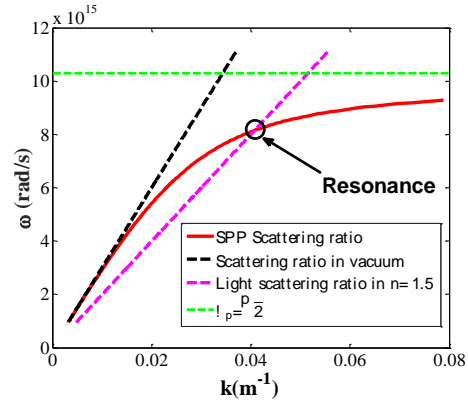


Figure 4. Scattering relation for propagating surface plasmons (red line), for light in vacuum (black dotted line), and for light in glass (magenta dotted line).

#### 1.4 Resonance of propagating surface plasmons

As mentioned above, surface plasmon resonance is a physical phenomenon that occurs when free electrons in a metallic film, usually Au or Ag, are excited by the incidence of polarized light. [21, 22] There are two configurations for this purpose, one by Otto and the other by Kretschmann.

##### 1.4.1 Otto's configuration

In this configuration a prism with high refractive index  $n_p$  is interconnected with a dielectric-metallic waveguide consisting of a dielectric thin film with refractive index  $n_d$  ( $n_p < n_d$ ) and thickness  $d$  and a semi-infinite metal with constant dielectric  $\epsilon_m$ . In this geometry, as shown in Fig.5, a light wave incident on the prism-dielectric film interface at an angle of incidence larger than the critical angle of incidence for these two media produces an evanescent wave propagating along the interface between the prism and the dielectric film. It is known that the nature of the evanescent wave has constant propagation along the interface and that it decays exponentially in the dielectric medium adjacent to the metallic film. Both characteristics of the evanescent wave are similar to those of a surface plasmon wave, therefore, there is a great possibility of interaction between these waves. [23, 24] However, this configuration is difficult to realize in practice, since the metal must be within  $\sim 200$  nm of the prism surface. This approach has been found to be very useful for studying single crystal metal surfaces and adsorption on them. [24]

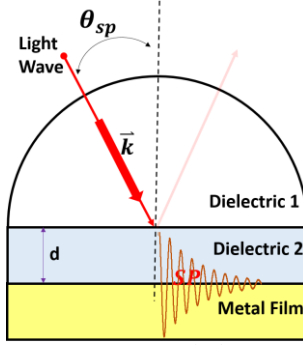


**Figure 5.** Modified Otto's optical configuration for the excitation of surface plasmons at the Dielectric2-Metal interface. Dielectric 1 is a cylindrical lens.

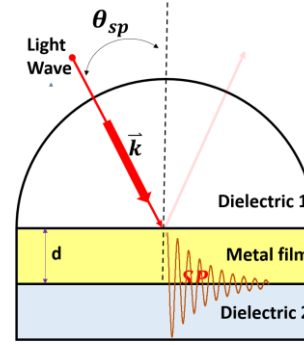


**Figure 6.** Modified Kretschmann's optical configuration for the excitation of surface plasmons at the Metal-Dielectric2 interface. Dielectric 1 is a cylindrical lens.

#### 1.4.2 Kretschmann's configuration

In this configuration, a prism with a high refractive index  $n_p$  is interconnected with a metal-dielectric waveguide that is formed by a metallic film with dielectric constant  $\epsilon_m$  and thickness  $d$  and a dielectric semifinite with a refractive index  $n_d$ . A resonance condition is that the refractive index of the dielectric to be measured is less than the refractive index of the prism  $n_d < n_p$ . This modified configuration is shown in Fig.6.

When a light wave propagating in the prism strikes the metallic film, part of the light is reflected back into the prism, the metallic film acting as a mirror, and part propagates in the metal in the form of a wave inhomogeneous electromagnetic. [23, 25] When the wave incident through the prism, then under conditions of total internal reflection, as the angle of incidence  $\theta_i$  changes, a certain angle is found at which the reflectivity decays. This decay is due to the fact that the photons of the light with electromagnetic polarization TM can interact with the free electrons of the metallic film, inducing an oscillation in the form of a wave of the free electrons, thus reducing the intensity of the reflected light. This angle of low reflectivity is known as the surface plasmon resonance angle and depends on the optical characteristics of the system, such as the refractive indices of the materials on both sides of the metal. [6, 23]

In order for this reflectivity decay to take place, the inhomogeneous wave decays exponentially in a direction perpendicular to the prism-metal interface and it is called an evanescent wave. If the metal is thin enough ( $\sim 50$  nm for visible light and part of the near infrared of the electromagnetic spectrum), the evanescent wave penetrates through the metal film and couples with a surface plasmon at the outer boundary of the methyl film. [23]

#### 1.5 Fresnel's equations in multilayer systems

To perform calculations of the reflected intensity at different angles of incidence, it is necessary to use the Fresnel equations in multilayer systems. These equations allow to simulate the resonance of the propagating surface plasmons. Fig.7 shows a schematic of the electromagnetic problem associated with the reflection and transmission of a wave from medium  $i$  to medium  $j$ . The parallel component of the wave vector  $\kappa_x$  is conserved when passing from one medium to another and can be calculated as:

$$\kappa_{xi} = \kappa_{xj} = \kappa_o n_i \sin(\theta_i) \quad (17)$$

Where  $\kappa_o = 2\pi/\lambda$  is the module of the wave vector in vacuum and  $n_i = \sqrt{\epsilon}$  the refractive index of medium  $i$ . The  $\kappa_z$  component in each medium can be obtained from the Pythagorean theorem.

$$\kappa_{zi} = \sqrt{\kappa_o^2 n_i^2 - \kappa_{xi}^2} \quad (18)$$

Taking into account Snell's law  $n_i \sin(\theta_i) = n_j \sin(\theta_j)$  in combination with the calculated components of the wave vector in each medium, the Fresnel's equations for the two types of polarization can be derived: TM polarization, if the B field is perpendicular to the plane of incidence; TE polarization, if the E field is perpendicular to the plane of incidence.

For polarization TE:

$$r_{ij}^s = \frac{\kappa_{zi} - \kappa_{zj}}{\kappa_{zi} + \kappa_{zj}}, \quad (19)$$

$$t_{ij}^s = \frac{2\kappa_{zi}}{\kappa_{zi} + \kappa_{zj}}, \quad (20)$$

For polarization TM:

$$r_{ij}^p = \frac{n_j^2 \kappa_{zi} - n_i^2 \kappa_{zj}}{n_j^2 \kappa_{zi} + n_i^2 \kappa_{zj}}, \quad (21)$$

$$t_{ij}^p = \frac{2n_i^2 n_j^2 \kappa_{zi}}{n_j^2 \kappa_{zi} - n_i^2 \kappa_{zj}}, \quad (22)$$

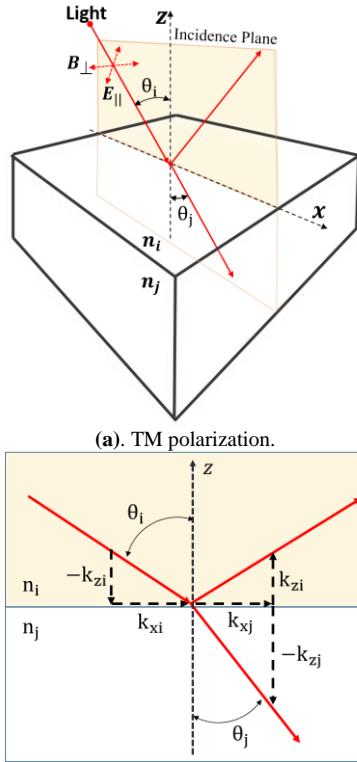
From these coefficients, assuming that there is no absorption, it is possible to calculate the intensity of the transmitted (T) and reflected (R) wave as:

$$R^x = r_{ij}^{x2} \quad (23)$$

$$T^x = 1 - R^x \quad (24)$$

Where  $x$  corresponds to either TM or TE polarization.

Using the Fresnel's equations, it is possible to do the calculation for a problem where there are more than two media. For this, the three-media problem is first solved as shown in Fig.8, where the only relevant spatial magnitude is the thickness  $d$  of media 1.



(b). Wave vector diagram on the plane of incidence.

**Figure 7.** Scheme of the electromagnetic problem of transmission and reflection of a wave through an interface between two materials.

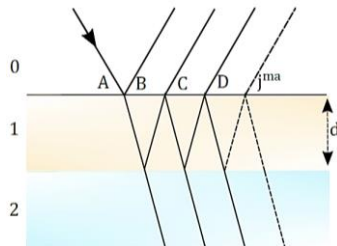


**Figure 8.** Diagram of the multiple reflections and interferences produced by the incidence of a plane wave in a system of three material media.

In this problem it is necessary to take into account the infinite reflections between the two interfaces and their respective transmissions which, in order to calculate the total reflected and transmitted waves, are computed as a geometric series

whose sum is reduced to a simple formula. Using the Fresnel's coefficients, the amplitude of the first reflection is  $B = r_{01}A$  and the transmission is  $t_{01}A$ . By considering the reflection of the transmitted wave at the second interface and its subsequent transmission at the first interface, the amplitude can be calculated of the partial wave C as:

$$C = t_{01}r_{12}t_{10}e^{(2ik_{z1}d)}A \quad (25)$$

where the factor  $e^{(2ik_{z1}d)}$  corresponds to the phase shift of the wave as a result of passing through medium 1. Similarly, the amplitude of the partial wave D can be calculated as:

$$D = t_{01}r_{12}^2r_{10}t_{10}e^{(2ik_{z1}d)^2}A \quad (26)$$

and finally, the  $j$ -th partial wave can be calculated as:

$$j^{ma} = t_{10}t_{01}r_{12}^j r_{10}^{j-1} e^{(2ik_{z1}d)j}A \quad (27)$$

Adding all the partial waves and dividing by the amplitude  $A$  of the incident wave, the effective Fresnel's coefficient  $r_{02}$  for the three-half problem can be obtained as:

$$r_{02} = r_{01} + t_{01}t_{10}r_{12}e^{(2ik_{z1}d)} \sum_{j=0}^{\infty} r_{12}^j r_{10}^j e^{(2ik_{z1}d)j} \quad (28)$$

Replacing the series by its sum, a simple form for the Fresnel's coefficient  $r_{02}$  is obtained:

$$r_{02} = r_{01} + \frac{t_{01}t_{10}r_{12}e^{(2ik_{z1}d)}}{1-r_{12}r_{10}e^{(2ik_{z1}d)}} \quad (29)$$

Then, applying the known relations for the Fresnel's coefficients  $r_{ij} = -r_{ji}$  and  $1+r=t$  [31], the effective reflection Fresnel coefficient can be expressed as:

$$r_{02} = \frac{r_{01}+r_{12}e^{(2ik_{z1}d)}}{1+r_{01}r_{12}e^{(2ik_{z1}d)}} \quad (30)$$

and the transmission as:

$$t_{02} = \frac{t_{01}t_{12}e^{(2ik_{z1}d)}}{1+r_{01}r_{12}e^{(2ik_{z1}d)}} \quad (31)$$

## 2. Resonance of propagating surface plasmons

Surface plasmon resonance is the resonant oscillation of conduction electrons at the interface between positive and negative permittivity material stimulated by incident light. The most efficient way to generate the propagating surface plasmons is the Kretschmann's configuration. A high refractive index prism is covered at its base with a metal film and the propagating surface plasmons are excited in the metal film by the mechanism of attenuated total reflection. The field of propagating surface plasmons decays exponentially below and above the limit, and the coincidence of the resonance condition, which is extremely sensitive to changes in the refractive index of the surrounding medium, is accompanied by a drop in power carried by the reflected light wave. Consequently, the surface plasmon resonance

phenomenon is manifested by changes in the intensity, phase, resonant angle, or resonant wavelength of the reflected light wave. Surface plasmon resonance is the fundamental principle of many biosensor applications. The Kretschmann's configuration is used, because in said configuration a coupling prism is used through which a light beam with TM polarization is incident that can be coupled with the surface plasmon present in the metal-dielectric interface due to the excitation of the free electrons present on the surface of such metal, especially Au or Ag. The propagating surface plasmons depend on the polarization mode. Some simulations are carried out that correspond to reflectivity maps with TM and TE polarization to show the resonance of propagating surface plasmons (see Fig.9).

### 2.1 Substrates used for propagating surface plasmon resonance

In the Kretschmann's configuration a coupling prism is used, for the present work a prism made of Bk7 glass is used. BK7 glass is one of the basic materials for the manufacture of optical details for lasers in the visible and near-infrared range. The refractive index of BK7 glass is 1.515 for a wavelength of 633 nm, which are the most used parameters in the simulations of this work. The metallic film is deposited on the BK7 glass for the respective tests. The film is generally adhered to the glass using the Sputtering technique in which it is deposited in a controlled manner in the order of nms. The substrates used in the Kretschmann's configuration are of a commercial type, the company (Platypus Technologies) is in charge of manufacturing said substrates. A BK7 glass slide (Fisher Scientific total area  $400 \text{ mm}^2$ ) is used as a substrate. [27] Glass slides are originally  $0.1 \text{ mm}$  thick, however they are too brittle to work with so it is convenient to use  $0.5 \text{ mm}$  thick slides for the substrate. [27]

Most of the companies that manufacture the samples for the surface plasmon resonance by the Kretschmann's configuration mainly use the Sputtering technique. There are various methods of film deposition which is a vacuum technology for applying coating of pure materials to the surfaces of various objects. Coatings typically range in thickness from Angstroms to microns and can be single material or multi-material in a layered structure. [27]

#### 2.1.1 Propagating surface plasmons and their dependence on polarization

To study the propagation of electromagnetic waves with TE and TM polarizations when propagating in a metal-dielectric interface, the wave equations must be satisfied by the fields that propagate in the system. For this it is assumed that the electromagnetic wave propagates in a single direction and also the wave propagates at the interface of the two media, so it can be defined that the dielectric function only varies when the medium changes, that is, that  $\epsilon = \epsilon(z)$ . [28]

In Fig.9 the reflectivity maps for the TM and TE polarizations are shown. In the reflectivity maps it is easy to see how the plasmons propagate on the surface and the angle of incidence where the excitation occurs. When a beam of light with TM polarization is incident on the surface of a metal film, there is a component of the electric field parallel to the surface which allows the excitation of the propagating surface plasmon, the thin line indicated in the Fig.9(a),(c) indicates the presence of the surface plasmon.

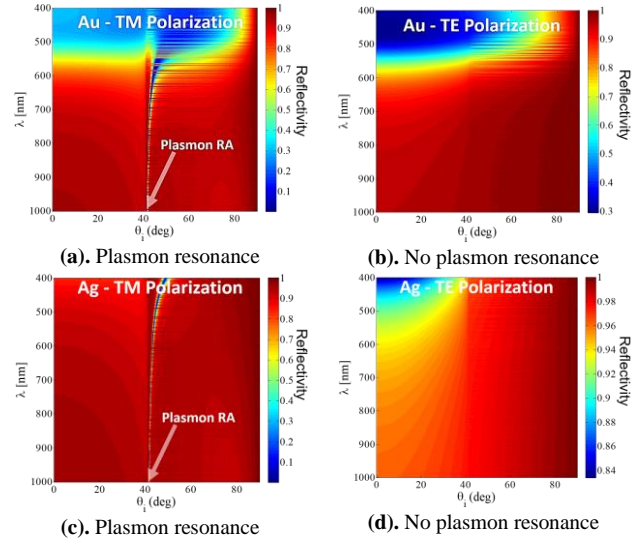


**Figure 9.** Reflectivity maps for the TM (a) and TE (b) polarizations. The scale of values corresponds to the following: red color at high reflectivity (low absorption) and blue color at low reflectivity (high absorption). The thin line within the reflectivity map indicates the existence of the propagating surface plasmon. Plasmon RA: Plasmon Resonance Angle.

To study the behavior of propagating surface plasmons in a metallic film using the Kretschmann's configuration with TM and TE polarizations, the following parameters were taken into account: a  $50 \text{ nm}$  metal film (Au or Ag), the dielectric function for the metal film, a BK7 glass prism and 3 air as medium. The Fresnel's coefficients Eq.(30)-(33) were used for these simulations.

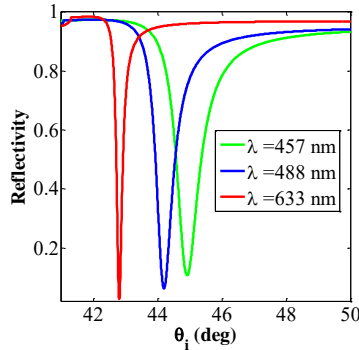
$$t_{12} = \frac{2\sqrt{\mu_2\epsilon_1}}{\sqrt{\mu_2\epsilon_1} + \sqrt{\mu_1\epsilon_2}} \quad (32)$$

$$r_{12} = \frac{\sqrt{\mu_2\epsilon_1} - \sqrt{\mu_1\epsilon_2}}{\sqrt{\mu_1\epsilon_2} + \sqrt{\mu_2\epsilon_1}} \quad (33)$$

For the reflectivity curve with TM polarization, the color scale corresponds to: red color for maximum reflectivity values (minimum in absorption) and blue color for minimum reflectivity values (maximum in absorption). In the TE polarization, Fig.9.(b),(d) it is considered that the magnetic field is parallel to the plane of incidence, therefore when the metallic film is illuminated with TE polarization there is no component of the electric field that propagates along the surface of the film, therefore there is no existence of surface plasmons in that direction. In the reflectivity map, a range of incidence angles of  $0-90^\circ$  was considered.

The Fig.10 are profiles taken from Fig.9(c). It can be seen from the simulation the presence of a minimum in intensity that corresponds to the resonance of the propagating surface plasmon.

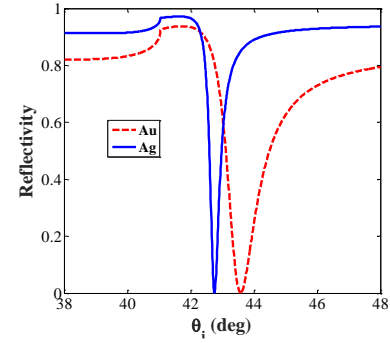
A 50 nm Au film was used, with BK7 prism with dielectric constant  $n_d = 1.523$  and  $\epsilon_a = 1$ . The exact positions that have both  $\theta_c$  (critical angle) and  $\theta_{sp}$  (surface plasmon angle) are also important at the time of plasmonic excitation. In the results obtained, it can be seen that for angles of incidence greater than the critical angle  $\theta_c$ , the reflectivity is less than in the case of total internal reflection due to a certain absorption in the metal and keeps decreasing until it approaches the coupling angle with the propagating surface plasmons, where the reflectivity takes the minimum value. As mentioned in previous sections, the propagating surface plasmons generate an optical field at the metal-dielectric interface which has its maximum intensity at said interface and decays exponentially towards the interior of the dielectric.



**Figure 10.** Theoretical model of the reflectivity curves for a 50 nm Ag film, for a BK7 prism. These profiles are taken from Fig.9(c).

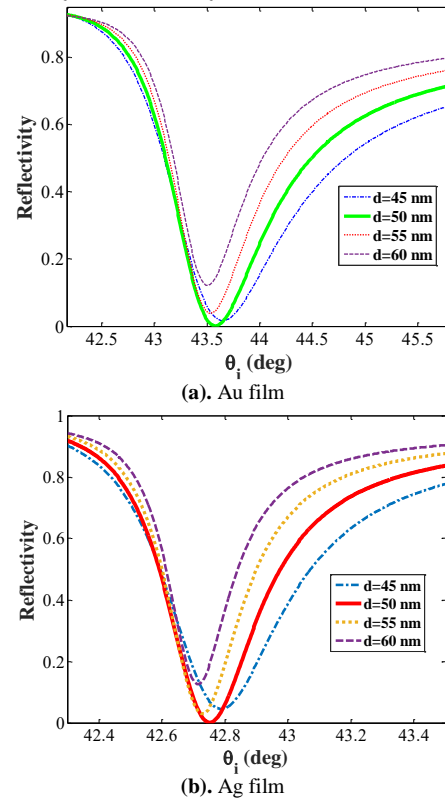
This also happens in the case of total internal reflection. Due to the resonance process that exists between the incident electromagnetic field and the propagating surface plasmons, there is an increase in the intensity of the evanescent field on the surface of the metallic film.

Fig.11 shows a calculation of reflectivity as a function of the angle of incidence in the Kretschmann's configuration using a 50 nm film for both Au and Ag. As it can be seen, the reflectivity remains very close to unity except for the angle where the incident light beam couples with the propagating surface plasmon, then the reflectivity drops sharply creating a very narrow valley and reaching zero where the surface plasmon excitation angle for Au is  $\sim 43.6^\circ$  while for Ag it is  $\sim 42.7^\circ$ . It can also be seen that the plasmon obtained for Ag is narrower in resonance than the Au plasmon, because Au is more chemically stable than Ag.



**Figure 11.** Reflectivity curve: for Au and Ag as a function of the angle of incidence with TM polarization and illumination  $\lambda = 633$  nm on a 50 nm Au and Ag film from a BK7 prism.

*2.1.2 Propagating surface plasmons and their dependence on the thickness of the metallic film*



**Figure 12.** Reflectivity curve for different thicknesses of the metallic film: a) for Au and b) for Ag. Air was used as medium 3, metallic film thicknesses of 45, 50, 55 and 60 nm were used for both metals, a prism BK7, the dielectric function used for the Au film corresponds to  $\epsilon = -11.42 + 1.186i$  for a wavelength of  $\lambda = 633$ nm. For the Ag film, the dielectric function used corresponds to  $\epsilon = -16.13 + 0.7494i$  for  $\lambda = 633$  nm.

Fig.12 shows a calculation of reflectivity vs the angle of incidence, for various thicknesses of the metallic film. In a) the results for an Au film and in b) for an Ag film are shown. For the simulation, the parameters used in previous sections were used.

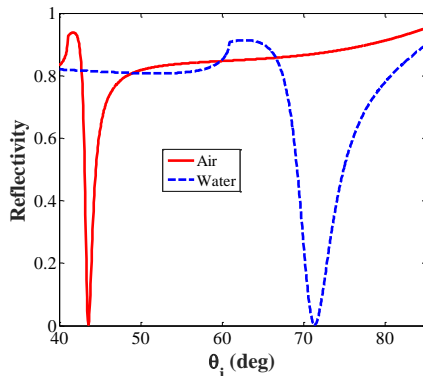
It can be seen that there is stability in the angle at which the plasmon resonance is generated, but the existence of a more



efficient configuration than the others to generate surface plasmons can be seen, that is, a thickness where the reflectivity presents a minimum more pronounced than the others, in the case of Au and Ag the optimum thickness is 50 nm. When the thickness of the metallic film is increased, the following situations occur: the plasmon resonance in the Au film becomes wider while for the plasmon of the Ag film the same width is maintained, in the same way that for in the Au film, the plasmon resonance undergoes a shift for larger angles and the displacement of the plasmon resonance in the Ag film is minimal.

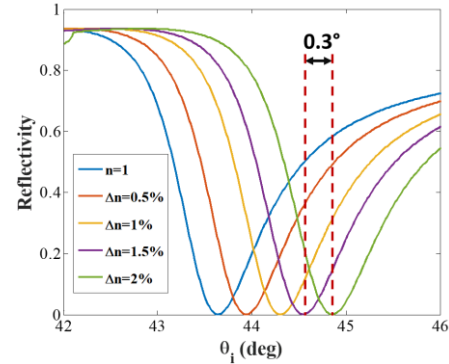
### 2.1.3 Dielectric refractive index dependent propagating surface plasmons

Fig.13 shows a calculation of reflectivity vs the angle of incidence by varying the refractive index of the dielectric medium: Fig.13.(a) Reflectivity curve for a plasmon with a propagating surface for which the dielectric medium is air; Fig.13.(b) the reflectivity curve for a propagating surface plasmon in which the dielectric medium is water. As it can be seen in Fig.13.(a), the resonance angle of the surface plasmon for the Au film whose dielectric medium is air is  $43.8^\circ$ , while the resonance angle for the propagating surface plasmon of the Au film whose dielectric medium is water is  $71.82^\circ$ , producing an increasing change of  $28.21^\circ$  in the angle of maximum resonance. What can be deduced from the reflectivity curves of these plasmons is that the surface plasmon resonance is susceptible to changes in the refractive indices of the dielectric media, for which this principle can be used for the operation of a molecule sensing.



**Figure 13.** Reflectivity curves for an Au film as a function of the angle of incidence whose dielectric medium 3 is air or water.

Likewise, in Fig.14 when the refractive indices of medium 3 (air) varied by 0.5%, there was an angular shift in each of the reflectivity curves of  $0.3^\circ$ . Verifying with this simulation that a good sensitivity of the technique is observed using the Kretschman's configuration, which if the (air) is taken into account as medium 3, this technique can serve as an operating principle for gas sensors.



**Figure 14.** Reflectivity as a function of the angle of incidence of an Au film with air dielectric medium 3, where this refractive index was varied at intervals of 0.5%.

These gas sensors or olfactory biosensors are single-sensor devices capable of detecting gases that consist of a receiver coupled to a transducer and a data processing system. The propagation of SPR with coupling configurations using a prism between them the Kretschmann's configuration are very efficient for such applications in the detection of volatile gases in either liquid or gaseous form. [29]

### 3. Conclusions

In the graphic representation of the real and imaginary parts of the dielectric function, the expression of the Drude's model was parameterized, where it is observed that the resonant absorption is reflected in the imaginary part of the dielectric function. When there is an approximation to the resonance frequency, the real part has a maximum that reflects the resonant increase in displacement. The negative real part of the dielectric function implies that the material will prevent wave penetration resulting in strong reflectivity. When simulating the dispersion relations for the propagating surface plasmon, for the light in a vacuum and for the light in the glass of the graph obtained, it was possible to verify that the propagating surface plasmons do not directly couple to an electromagnetic field incident from the vacuum, hence the need to use a coupling prism with a high refractive index using the Kretschmann's configuration.

In this investigation, it was verified that the resonance of surface plasmons depends on the TM and TE polarization; in the reflectivity maps of Au and Ag, for example, it is observed that only in the TM configuration it is possible to generate the excitation of the surface plasmon, while when the electric field is polarized perpendicularly to the plane of incidence (TE) the excitation does not occur of the surface plasmon. In the Kretschmann's configuration, the dependence on the thickness of the metal film, it was found that the surface plasmon resonance is highly sensitive to this parameter; e.g. for Au the optimal thickness found was 50 nm and for Ag and Au. As the thickness of the metal film increases, e.g. using Au, the mean width of the valley of the

reflectivity curve increases, while using Ag film the mean width of the valley of the reflectivity curve remains constant. Another aspect studied and to highlight is the dependence on the wavelength of light, finding an important difference between using Au or Ag; in the first case the SPR is presented in a bandwidth of  $\sim 662$  nm to 1000 nm; while using Ag, the SPR was observed in a bandwidth of  $\sim 400$  nm to 1000 nm.

Regarding the dependence of the refractive index of medium 3, it was found that minimal variations of the refractive index (e.g. 0.5%) cause a detectable shift ( $0.3^\circ$ ) to occur in the resonance angle of the surface plasmon; it was confirmed that the Kretschmann configuration can be used in the construction of olfactory sensors or to monitor the purity or changes in liquid substances. With this study we want to show the real potentialities of using the SPR phenomenon in the construction of highly sensitive optical sensors.

## References

- [1] Schasfoort, R. B., Lokate, A. M., Beusink, J. B., Puijn, G. J., Engbers, G. H. Measurement of the analysis cycle: Scanning spr microarray imaging of autoimmune diseases. En: Handbook of Surface Plasmon Resonance, pags. 221-245. Royal Society of Chemistry, 2008.
- [2] Knoll, Wolfgang. Interfaces and thin films as seen by bound electromagnetic waves. Annual review of physical chemistry, 1998.
- [3] Sepúlveda Borja Regatos, David Armelles Reig, Gaspar Lechuga, Laura M and Fariña David. Método para el análisis del índice de refracción de un medio dieléctrico adyacente a un medio plasmónico, y dispositivo correspondiente. Oficina española de patentes y marcas, 2011.
- [4] Cesar Aurelio Herreño Fierro. Magneto plasmónica de estructuras multicapa Au|Co|Au. Universidad de los Andes, 2015.
- [5] Le Ru, E., Etchegoin, P. Principles of Surface-Enhanced Raman Spectroscopy: and related plasmonic effects. Elsevier, 2009.
- [6] Maier, S. A. Plasmonics: fundamentals and applications. Springer Science & Business Media, 2007.
- [7] Rojas Bejarano, Carlos Javier and others. Resonancia de plasmones superficiales localizados en nanopartículas de oro y plata. Universidad Distrital Francisco José de Caldas, 2020.
- [8] Fox, Mark. Optical properties of solids. American Association of Physics Teachers, 2002.
- [9] Guerra Hernández, L. A. Antenas ópticas en la nano y micro escala. Tesis Doctoral, Universidad Nacional de Cuyo, 2019.
- [10] Bonanca, M. V., Nazé, P., Deffner, S. Negative entropy production rates in Drude Sommerfeld metals. Physical Review E, 103 (1), 012109, 2021.
- [11] Wood, R. W. Xlii. on a remarkable case of uneven distribution of light in a diffraction grating spectrum. The London, Edinburgh, and Dublin Philosophical Magazine and Journal of Science, 4 (21), 396-402, 1902.
- [12] Daniel Schinca, Lucia Scafardi. Plasmónica. Centro de investigaciones ópticas, 2011.
- [13] Cubillos Morales, Fabián Camilo. Resonancia de plasmón superficial en películas delgadas de ZnO. Universidad Tecnológica de Pereira, 2017.
- [14] Guerra Hernández, L. A., Daza Millone, M. A., Cortés, E., Castez, M. F., Auguie, B., Vela, M. E., et al. Synergetic light-harvesting and near-field enhancement in multiscale patterned gold substrates. ACS Photonics, 2 (9), 1355-1365, 2015.
- [15] Pines, D. Collective energy losses in solids. Reviews of modern physics, 28 (3), 184, 1956.
- [16] Jackson, J. D. Classical Electrodynamics. ed. Wiley, New York, 1999.
- [17] Barker Jr, A. Optical measurements of surface plasmons in gold. Physical Review B, 8 (12), 5418, 1973.
- [18] Raether, H. Surface plasmons on smooth surfaces. En: Surface plasmons on smooth and rough surfaces and on gratings, págs. 4-39. Springer, 1988.
- [19] Sambles, J., Bradbery, G., Yang, F. Optical excitation of surface plasmons: an introduction. Contemporary physics, 32 (3), 173-183, 1991.
- [20] Yannopoulos, V., Stefanou, N. Optical excitation of coupled waveguide-particle plasmon modes: A theoretical analysis. Physical Review B, 69 (1), 012408, 2004.
- [21] Goñi Olóriz, Carlos. Camino de la resonancia de plasmón superficial en fibra óptica pulida lateralmente. Universidad Pública de Navarra, 2010.
- [22] Interaxn S.L. Informe de vigilancia tecnológica sobre aplicación de biosensores al diagnóstico simultáneo de enfermedades infecciosas. Tesis Doctoral, Fundación para el conocimiento madrid, 2004.
- [23] Sanchez, Y. M. E. Automatización de un sistema de resonancia de plasmones de superficie para medición de índice de refracción. Tesis Doctoral, Centro de investigación óptica A. C., 2013.
- [24] Sharma, A. K., Jha, R., Gupta, B. Fiber-optic sensors based on surface plasmon resonance: a comprehensive review. IEEE Sensors Journal, 7 (8), 1118-1129, 2007.
- [25] Homola, J., Piliarik, M. Surface plasmon resonance (SPR) sensors. En: Surface plasmon resonance based sensors, págs. 45-67. Springer, 2006.
- [26] Stenzel, O., et al. The physics of thin film optical spectra. Springer, 2015.
- [27] Hma Salah, Nasih. Surface Plasmon Resonance Sensing and Characterisation of Nano-Colloids for Nanotoxicology Applications. Plymouth University, 2015.
- [28] Cárdenas, M., Castiblanco, R. E., Vargas, J. H., Morales, J. Estudio de las funciones reflectancia y transmitancia de los plasmones de superficies en la configuración de kretschmann. Momento, (40), 30-55, 2010.
- [29] El Kazzy Marielle, Weerakkody Jonathan, Hurot Charlotte, Mathey Raphael, Buhot Arnaud, Scaramozzino Natale, Hou Yanxia. An Overview of Artificial Olfaction Systems with a Focus on Surface Plasmon Resonance for the Analysis of Volatile Organic Compounds. Biosensors, 2021.
- [30] Gélvez L-Edison., Rueda Jorge-Enrique, Guerra Luis-A., Resonancia de plasmones de superficie en sistemas films metálicos. Trabajo de grado Física, Universidad de Pamplona, 2022.